JOURNAL OF PROPULSION AND POWER
Vol. 22, No. 1, January–February 2006

Design of Control Law for Rotating Stall Subject to Actuator Constraints

Craig A. Buhr,* Matthew A. Franchek,† and Sanford Fleeter‡
Purdue University, West Lafayette, Indiana 47907

Presented in this paper is an analytical study of the closed-loop stability of rotating stall control in an axial flow compressor subject to a nonlinear spatial actuation constraint. To account for the actuator constraints during the design, the problem is formulated as an absolute stability problem for a linearized spatial domain model of an axial flow compressor in series with the saturation element. In particular, the circle criterion is extended to accommodate the complex nature of the spatial domain. A graphical interpretation of the circle criterion results, which allows classical control design techniques to be used in the design of the gain and phase for a complex gain control law that increases the region of absolute stability guaranteed by this closed-loop system-stability criteria. This allows for the actuator constraints to be accounted for during the design using classical control techniques. A comparison of the estimated domain of attraction from the circle criterion and the domain of attraction obtained through simulation of the full nonlinear compressor model are presented.

Nomenclature

A_r	=	ratio of injector area to compressor duct area
B	=	Greitzer B-parameter
$G(s)$	=	open-loop linear transfer fuction
k	=	complex gain control law gain
L_r	=	unsteady losses across the rotor
L_s	=	unsteady losses across the stator
n	=	spatial mode number
β	=	complex gain control law phase
γ_n	=	saturation level
θ	=	circumferential position
λ	=	rotor fluid inertia parameter
μ	=	compressor fluid inertia paramter
τ_a	=	actuator time constant
τ_r	=	rotor unsteady loss time constant
τ_s	=	stator unsteady loss time constant
ϕ_3	=	flow coefficient at inlet of compressor
ϕ_j	=	injection flow coefficient
ϕ_{jc}	=	injection command
Ψ_{isen}	=	isentropic compressor characteristic
$\Psi(\cdot,\cdot)$	=	nonlinearity
$(\hat{\cdot})_n$	=	nth Fourier coefficient
$(\bar{\cdot})$	=	mean value
$(\cdot)^*$	=	complex conjugate transpose

I. Introduction

ACTUATOR constraints such as magnitude saturation and rate saturation can limit achievable closed-loop performance and stability as predicted by linear system theory. Thus, closed-loop performance and stability cannot be assessed with linear system theory unless the actuator never saturates. Stability criteria such as the circle criterion and Lyaponov-based methods can be used to incorporate actuator nonlinearities in controller design. In this study, an extension of the circle criterion is incorporated in the design of a control law for rotating stall subject to actuator saturation.

Peak performance and efficiency of compressors often occur at operating points near the surge line. The surge line is the boundary between stable and unstable (rotating stall and/or surge) compressor operation under ideal conditions. Rotating stall and surge are aerodynamic instabilities that degrade compressor performance and produce large loading effects on the compressor blades. To ensure stable compressor operation despite less than ideal conditions such as external disturbances and component deterioration, the compressor is operated at conditions removed from the surge line (surge margin). Thus, peak performance and efficiency are sacrificed to guarantee stable operation.

In an attempt to reduce the surge margin required to ensure stable operation, active feedback control schemes have been developed for the control of rotating stall. Two-dimensional actuation/sensing feedback control schemes refer to the use of distributed sensing to measure spatial flow perturbations in the compressor, which provides the feedback signal for corrective spatial actuation. These schemes have been successful at improving compressor behavior at operating points near the surge line as well as extending the stable operating range of the compressor. For example, Protz[1] used a feedback linearization technique to design a controller for rotating stall with air injectors for actuation in which actuator saturation limited the domain of asymptotic stability. A more common feedback control law used for two-dimensional actuation for low-speed compressors is $u = k\exp(j\beta)y$. This control law is a proportional controller composed of a complex gain where the flow perturbation created by the two-dimensional actuation u is the sensed spatial harmonic y augmented in magnitude k and shifted in phase β.

The design of a complex gain controller can be pursued through a heuristic design approach or a model-based design technique. The heuristic approach uses an array of sensors around the annulus of the compressor to detect mass flow deficits. Knowing the approximate rate at which the mass flow deficit rotates around the annulus, a suitable phase shift is used such that the mass flow deficit will be in close proximity to the actuator used to energize the flow. Examples using arrays of solenoid-actuated air injectors for control using this type of control scheme can be found in Refs. 2–4. Another method of designing a complex gain controller is based on the evolution of small-amplitude circumferential traveling waves that arise prior to the development of rotating stall as predicted by the Moore and Greitzer model.[5] The parameters of the control law are commonly designed by stabilizing the closed-loop eigenvalues of the linearized version of the Moore Greitzer compressor model for this feedback system. Examples of control based on a linearized compressor model using movable inlet guide vanes for actuation

Presented as paper 2000-3505 at the AIAA/ASME/SAE/ASEE 36th Joint Propulsion Conference, Huntsville, AL, 16–19 July 2000; received 21 July 2004; revision received 15 July 2005; accepted for publication 20 July 2005.

*Research Assistant, School of Mechanical Engineering.
†Professor, School of Mechanical Engineering.
‡McAllister Distinguished Professor, School of Mechanical Engineering. Associate Fellow AIAA.

can be found in Refs. 6–8 and using air injectors for actuation can be found in Ref. 9. Several actuator/sensor schemes including the effect of actuator bandwidth for the control of rotating stall with a complex gain control law are detailed by Hendricks and Gysling.[10]

The purpose of this paper is to incorporate the spatial domain actuation magnitude limits on the complex gain control law design process. In particular, a design process is developed in this paper for the selection of k and β subject to actuation magnitude limits where the nonlinear element is defined in the spatial domain. The study is performed on a linearized spatial domain compressor model in series with a memoryless nonlinear element representing the actuation constraint.

To this end, the paper contains the following sections. First, background on the circle criterion is presented. Then, the problem is defined. The linearized spatial domain compressor model is then developed. In the following section, a review of the circle criterion and domains of attraction are presented. The modified circle criterion is then presented and applied to the compressor model. From this analysis the design of the control parameters is developed. The paper ends with a design example and conclusions.

II. Background

Absolute stability guarantees global (local) asymptotic stability for the class of systems shown in Fig. 1 where the nonlinearity is memoryless and globally (locally) sector bounded. Methods such as the circle criterion and Popov criterion provide sufficient conditions for absolute stability.[11,12] The Popov criterion differs from the circle criterion in that it restricts the sector-bounded nonlinearity to be time invariant. Thus, the circle criterion addresses a larger class of nonlinear feedback systems for absolute stability and can be more conservative for time-invariant nonlinearities.

For the case of local asymptotic stability, it is beneficial to determine the region about the equilibrium point such that all trajectories in this region converge to the equilibrium. This region is commonly referred to as the domain of attraction. An estimate of the domain of attraction can be derived by finding an attractive invariant subspace and serves as a measure of performance. Methods for calculating estimates of the domain of attraction can be found in Refs. 12–14.

A brief review of the multivariable circle criterion and the estimation of the domain of attraction is presented. For a more detailed discussion of these topics see Ref. 12.

A. Absolute Stability

The circle criterion provides sufficient conditions that guarantee global (local) absolute stability for the class of feedback systems depicted in Fig. 1 described by

$$\dot{x}(t) = Ax(t) + Bu(t) \tag{1}$$

$$y(t) = Cx(t) \tag{2}$$

$$u(t) = -\Psi(t, y) \tag{3}$$

where $x \in R^n$, $u, y \in R^p$, $A \in R^{n\times n}$, $B \in R^{n\times p}$, $C \in R^{p\times n}$, and the nonlinear element in the feedback path is memoryless and satisfies the sector-bound condition of definition 1 globally (locally).

Definition 1, Sector-Bounded Nonlinearity: A memoryless nonlinearity $\Psi(\cdot,\cdot) : [0,\infty) \times R^p \to R^p$ is said to satisfy a sector condition if $\forall\, t \geq 0$, $\forall\, y \in \Gamma \subset R^p$, and

$$[\Psi(t, y) - K_{\min} y]^T [\Psi(t, y) - K_{\max} y] \leq 0 \tag{4}$$

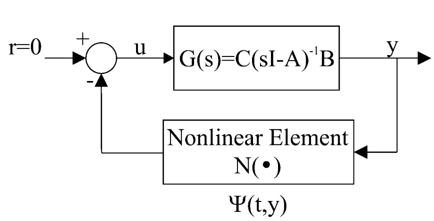

Fig. 1 Feedback system.

for some real matrices $K_{\min}$ and $K_{\max}$ where $K = K_{\max} - K_{\min}$ is a positive definite symmetric matrix and the interior of Γ is connected and contains the origin. If $\Gamma = R^p$ then $\Psi(\cdot,\cdot)$ satisfies the sector condition globally.[12]

Theorem 1, Multivariable Circle Criterion: Consider the system given by Eqs. (1)–(3), where (A, B) is controllable, (A, C) is observable, and $\Psi(\cdot,\cdot)$ satisfies the sector condition Eq. (4) globally. Then, the system is absolutely stable if

$$G_T(s) = G(s)[I + K_{\min} G(s)]^{-1} \tag{5}$$

is Hurwitz and

$$Z_T(s) = I + (K_{\max} - K_{\min}) G(s)[I + K_{\min} G(s)]^{-1} \tag{6}$$

is strictly positive real where

$$G(s) = C(sI - A)^{-1} B \tag{7}$$

is the transfer function matrix representation for the linear system given in Eqs. (1)–(2). If Eq. (4) is satisfied only on a set $\Gamma \subset R^p$, then the conditions given on $G_T(s)$ and $Z_T(s)$ ensure that the system is absolutely stable with a finite domain.[12]

B. Domain of Attraction

Domains of attraction are often estimated from a Lyapunov function. Lyapunov functions allow the stability of a system to be assessed without directly solving the equations of the system. For the system in Eqs. (1)–(3), the circle criterion provides sufficient conditions that a $P > 0$ exists such that $\dot{V}(x) < 0\, \forall\, x \in \{x \in R^n : y = Cx \in \Gamma\}$ for the Lyapunov function $V(x) = x^T P x$. Applying the following theorem to this Lyapunov function provides an estimate of the domain of attraction.

Theorem 2, Invariant and Attractive Set: Consider the system $\dot{x} = f(t, x)$. Suppose there is a continuously differentiable function $V(x)$, a continuous function $W(x)$, and a scalar c such that 1) $V(x)$ is radially unbounded and 2) $W(x)$ is such that

$$\dot{V}(x) \leq 0 - W(x) < 0 \quad \forall t \qquad \text{when} \quad V(x) < c$$

Then, the set $\Omega_c = \{x \in R^n : V(x) \leq c\}$ is an invariant and attractive set for the system $\dot{x} = f(t, x)$.[12]

Using Theorem 2 an estimate of the domain of attraction, denoted as $\Omega_c = \{x \in R^n : V(x) \leq V_\Gamma\}$, for the system in Eqs. (1)–(3) satisfying either the circle criterion can be determined by solving

$$V_\Gamma = \min_{x \in \Lambda} V(x)$$

where

$$\Lambda = \left\{x \in R^n : y = Cx \in \Gamma_B\right\}$$

and Γ_B is the boundary of Γ defined in Eq. (4).

III. Problem Statement and Actuation Constraint Description

Consider the spatial domain feedback control problem of extending the stable operating range for a low-speed axial flow compressor system through the feedback control of rotating stall. A pictorial representation of the compressor is shown in Fig. 2 with distributed sensing [output $y(t,\theta)$] and actuation [input $u(t,\theta)$]. The output and input are decomposed into its spatial Fourier harmonics:

$$y(t,\theta) = \sum_{n=1}^{\infty} \mathrm{Re}\left(\hat{y}_n^*(t) e^{in\theta}\right), \qquad u(t,\theta) = \sum_{n=1}^{\infty} \mathrm{Re}\left(\hat{u}_n^*(t) e^{in\theta}\right)$$

where $\hat{y}_n(t)$ and $\hat{u}_n(t)$ are the nth spatial Fourier coefficients of the output and input, respectively; θ is the annular circumferential position; and $*$ is the complex conjugate transpose operator. Utilizing this decomposition, a decoupled linear compressor model (presented in the following section) is developed relating the nth spatial mode input $u_n(t,\theta) = \mathrm{Re}\{\hat{u}_n^*(t) e^{in\theta}\}$ to the nth spatial mode

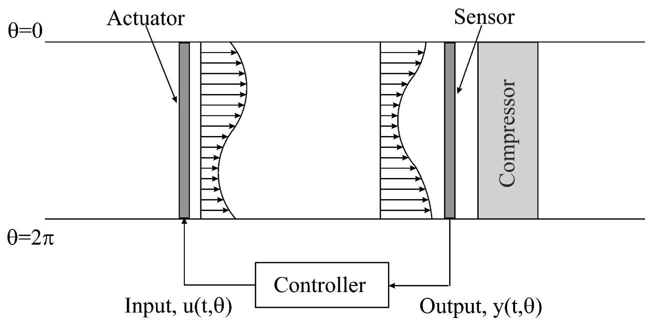

Fig. 2 Pictorial representation of compressor.[10]

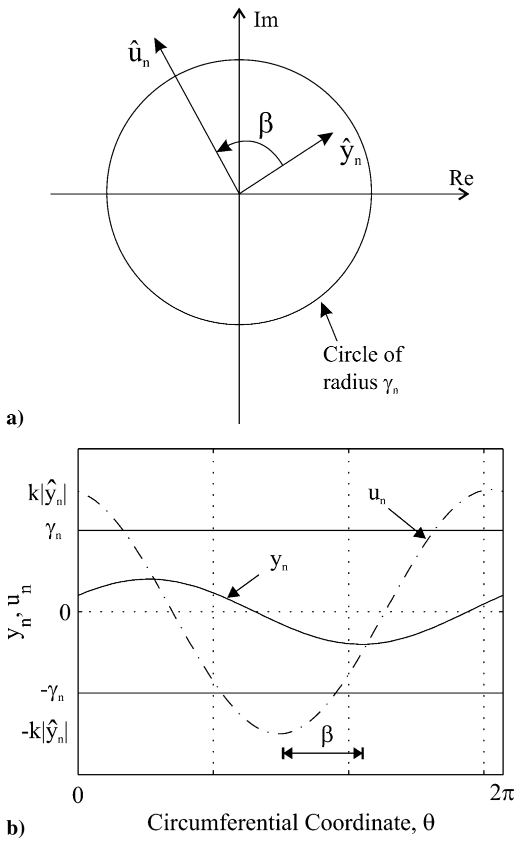

Fig. 3 Control without actuation constraint: a) vector representation and b) distributed actuation for $n = 1$.

output $y_n(t, \theta) = \mathrm{Re}\{\hat{y}_n^*(t)e^{in\theta}\}$. This realization of the compressor model allows an individual spatial mode to be treated as a SISO (single-input/single-output) regulator control problem.

Now, consider the complex gain control law

$$\hat{u}_n(t) = k_n e^{i\beta_n}\hat{y}_n(t) \tag{8}$$

for actuation of the nth spatial mode subject to a magnitude constraint γ_n. This actuator constraint limits the maximum amplitude of a spatial mode input as

$$\hat{u}_{n,\mathrm{sat}}(t) = \frac{\mathrm{sat}(|\hat{u}_n(t)|)}{|\hat{u}_n(t)|}\hat{y}_n(t) \tag{9}$$

where

$$\mathrm{sat}(\alpha) = \begin{Bmatrix} \alpha & \text{if} & \alpha \le \gamma_n \\ \gamma_n & \text{if} & \alpha > \gamma_n \end{Bmatrix} \tag{10}$$

An illustration between the cases without and with the actuation constraint is presented Figs. 3 and 4, respectively. Shown in Fig. 3 is the case without the actuation constraint. The vector representation

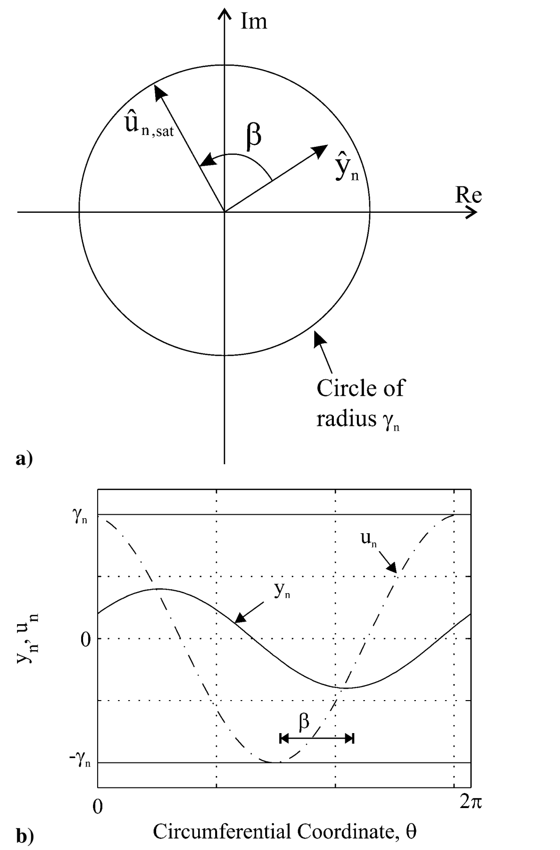

Fig. 4 Control with actuation constraint γ: a) vector representation and b) distributed actuation for $n = 1$.

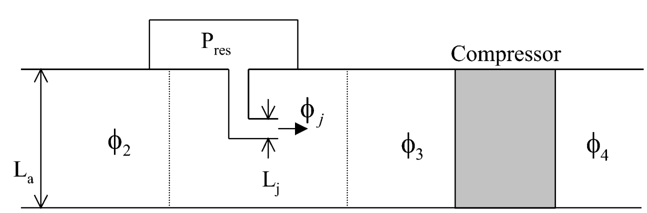

Fig. 5 Pictorial representation of compressor for modeling.[10]

in Fig. 3a illustrates the rotation β_n and amplification k_n of the output spatial mode vector $\hat{y}_n$ by the complex gain control law resulting in the input spatial mode vector $\hat{u}_n$. The resulting distributed representation of this control action for $n = 1$ is shown in Fig. 3b. Similarly consider the same control law with the actuation constraint given by Eq. (9) shown in Fig. 4. As shown in Fig. 4a, the control law rotates the output spatial mode vector $\hat{y}_n$; however, the amplification of the output vector is limited to γ_n because $k_n|\hat{y}_n| > \gamma_n$, resulting in the spatial mode output vector $\hat{u}_{n,\mathrm{sat}}$. The resulting distributed representation of this control action for $n = 1$ is shown in Fig. 4b.

The objective is to develop a method for designing a stabilizing complex gain feedback controller to extend the operating range of the compressor subject to a spatial actuator magnitude constraint. The design goal is to maximize the region of stability for a given level of actuation using the estimated domains of attraction from the modified circle criterion for the measure of performance.

IV. Linearized Model of the Compressor

Consider a compressor equipped with air injection for actuation and flow sensors. Shown in Fig. 5 is a representation of the compressor with air injectors for control.[10] A nonlinear compressor model is developed in a similar manner as presented in Behnken.[3] Linearization of this model about the mean flow rate $\bar{\phi}_3$ and mean injection rate $\bar{\phi}_j$ results in the following spatial domain compressor model given by

$$\dot{x}_n(t,\theta) = F x_n(t,\theta) + \begin{bmatrix} \dfrac{A_r}{\zeta|n|\tau_a} \\ \dfrac{1}{\tau_a} \\ 0 \\ 0 \end{bmatrix} \hat{u}_n(t,\theta)$$

$$\hat{y}_n(t,\theta) = [1 \quad 0 \quad 0 \quad 0] x_n(t,\theta) \tag{11}$$

where

$$F = \begin{bmatrix} \dfrac{1}{\zeta}\left(\dfrac{d\Psi_{\text{isen}}}{d\phi_3}\bigg|_{\bar{\phi}_3} - A_r\bar{\phi}_j + in\lambda\right) & -\dfrac{A_r}{\zeta}(2\bar{\phi}_j - \bar{\phi}_3 + A_r\bar{\phi}_j) - \dfrac{A_r}{\zeta|n|\tau_a} & -\dfrac{1}{\zeta} & -\dfrac{1}{\zeta} \\ 0 & -\dfrac{1}{\tau_a} & 0 & 0 \\ \dfrac{1}{\tau_r}\dfrac{dL_{\text{rs}}}{d\phi_3}\bigg|_{\bar{\phi}_3} & 0 & -\left(in + \dfrac{1}{\tau_r}\right) & 0 \\ \dfrac{1}{\tau_s}\dfrac{dL_{\text{ss}}}{d\phi_3}\bigg|_{\bar{\phi}_3} & 0 & 0 & -\dfrac{1}{\tau_s} \end{bmatrix}$$

$$x_n(t,\theta) = \left[\hat{\phi}_{3_n} \quad \hat{\phi}_{j_n} \quad \hat{L}_{r_n} \quad \hat{L}_{s_n}\right]^T, \qquad \zeta = \left(\frac{2}{|n|} + \mu\right)$$

$$A_r = \frac{L_j}{L_a}, \qquad L_{rs}(\phi_3) = (\Psi_{\text{isen}} - \Psi_{\text{css}})R$$

$$L_{\text{ss}}(\phi_3) = (\Psi_{\text{isen}} - \Psi_{\text{css}})(1-R)$$

The model represents the relationship between the nth spatial mode output and the nth spatial mode input. The input $\hat{u}_n(t) = \hat{\phi}_{jc}$ is the commanded injection rate. The output $\hat{y}_n(t) = \hat{\phi}_{3_n}$ is the nth spatial harmonic of the flow perturbation at the inlet of the compressor. The operating point is set by the mean flow coefficient $\bar{\phi}_3$. The mean injection rate $\bar{\phi}_j$ is chosen to be 2% of the stall mass flow rate $\bar{\phi}_{3,\text{stall}}$. The isentropic pressure characteristic is denoted by $\Psi_{\text{isen}}(\phi)$. The unsteady pressure losses across the rotors and stators are denoted by L_r and L_s, respectively. The parameters for the compressor are based on the compressor C2 in Mansoux et al.[15] (see Table 1). Compressor model maps are as follows:

$$\Psi_{\text{isen}}(\phi) = -15.5341\phi^3 + 24.1238\phi^2 - 15.0262\phi + 4.6951$$

$$\Psi_{\text{css}}(\phi) =$$

$$\begin{cases} 12.117\phi^2 - 2.423\phi + 0.221 & \phi \le 0.1 \\ -49.624\phi^3 + 39.509\phi^2 - 6.413\phi + 0.395 & 0.1 < \phi \le 0.4 \\ -10.0695\phi^2 + 9.430\phi - 1.184 & 0.4 < \phi \end{cases}$$

Table 1 Compressor model parameters

Variable	Value
$\phi_{3,\text{stall}}$	0.460
ϕ_j	0.467
B	0.1
μ	1.29
m	2
R	0.75
τ_s	0.37
τ_r	0.37
τ_a	0.1
λ	0.68
l_c	6.66
l_i	2.99
A_r	0.0197

V. Main Results

This work is concerned with extending the stable operating range of the compressor using the feedback control law, Eq. (8), subject to the actuation constraint of Eq. (9). The study is performed on a linearized compressor model in series with a memoryless nonlinear element representing the actuation constraint. Closed-loop stability for this feedback structure can be addressed using absolute stability theory.

A. Modified Circle Criterion

One of the benefits of the circle criterion is that for SISO systems there is a graphical interpretation. This graphical interpretation manifests itself as a constraint when using classical linear controller design techniques of loop shaping. Thus, stability with respect to the sector-bounded nonlinearity can be guaranteed using classical control techniques during the design. However, because the circle criterion applies to real coefficient models, a modified circle criterion is developed to facilitate the design process.

Definition 2, Disc $D(k_{\min}, k_{\max})$: A disc $D(k_{\min}, k_{\max})$ is a circle in the s-plane with diameter $(-1/k_{\max} + 1/k_{\min})$ and center at $(-1/k_{\max} - 1/k_{\min})/2$.

Theorem 3, Modified Circle Criterion: Consider the feedback system depicted in Fig. 1:

$$\dot{x}(t) = Ax(t) + Bu(t) \tag{12}$$

$$y(t) = Cx(t) \tag{13}$$

$$u(t) = -\Psi(t, y) = -\tilde{\Psi}(t, y)y \tag{14}$$

where $x \in C^n$, u, $y \in C^1$, (A,B) is controllable, (A,C) is observable, $G(s) = C(sI - A)^{-1}B$ is the transfer function of the linear element, and $\tilde{\Psi}(\cdot,\cdot) : [0,\infty) \times C^1 \to R^1$ is a memoryless nonlinearity satisfying $0 \le k_{\min} < \tilde{\Psi}(t, y) < k_{\max}$. Then, the system is absolutely stable if either of the following is satisfied:

1) If $0 = k_{\min} < k_{\max}$, $G(s)$ is Hurwitz and the polar plot of $G(j\omega)$ lies to the right of the vertical line defined by $\text{Re}\{s\} = -1/k_{\max}$.

2) If $0 < k_{\min} < k_{\max}$, the polar plot of $G(j\omega)$ does not enter the disk $D(k_{\min}, k_{\max})$ and encircles the disk counterclockwise n times, where n is the number of poles of $G(s)$ with positive real parts.

If the condition $0 \le k_{\min} < \tilde{\Psi}(t, y) < k_{\max}$ is satisfied only on a set $\Gamma \subset C^1$, then the conditions ensure that the system is absolutely stable with a finite domain.

Proof: See Appendix.

B. Formulation of the Feedback Structure for Circle Criterion

Shown in Fig. 6 is the block-diagram representation of the feedback control structure for the compressor with a complex gain control law subject to a nonlinear actuation constraint. Before the modified circle criterion can be applied, the block diagram in Fig. 6 must be formulated into the feedback structure shown in Fig. 1. Consequently, the gain k_n of the control law will be included in the nonlinear element, giving

$$\Psi(w_n) = \frac{\text{sat}(k_n|w_n(t)|)}{|w_n(t)|} w_n(t) \tag{15}$$

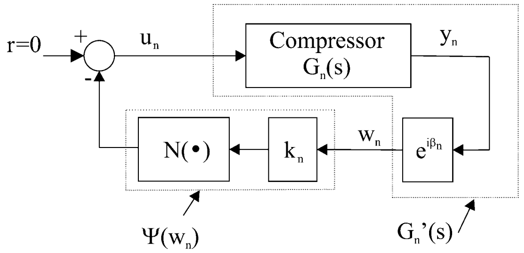

Fig. 6 Formulation of compressor control problem for application of the modified circle criterion.

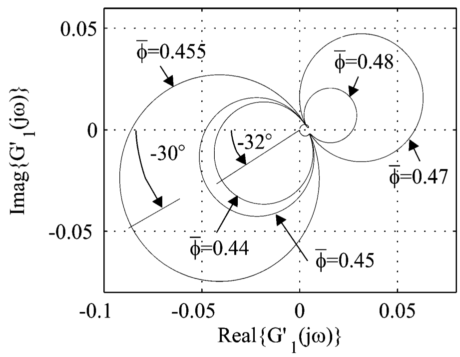

Fig. 7 Frequency response of $G_1'(s)$ with $\beta = 0$ deg.

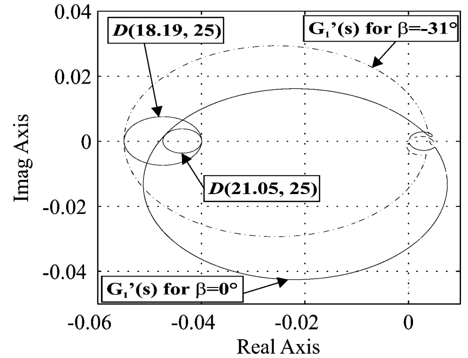

Fig. 8 Frequency responses of $G_1'(s)$ with $\beta = 0$ deg, —, and $\beta = -31$ deg, —·, $\phi = 0.45$.

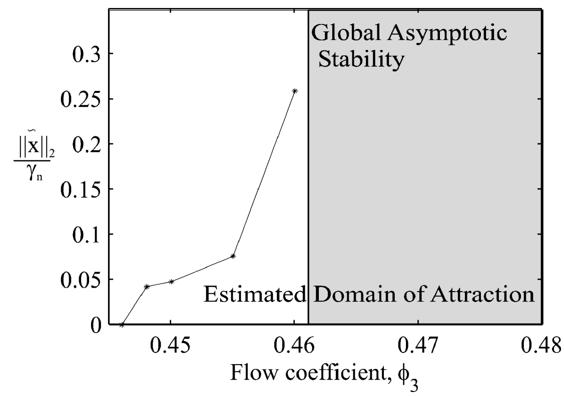

Fig. 9 Norm-bounded subset of Ω_{V_Γ}.

where sat(·) is defined in Eq. (10) and can be locally sector bounded on the set

$$\Gamma = \left\{ w_n \in C^1 : \|w_n\|_2 \le \gamma_n / k_{\min} \right\} \tag{16}$$

where $k_{\max} \ge k_n > k_{\min}$. The spatial phase shift β_n of the control law is included with the compressor dynamics as

$$\frac{W_n(s)}{U_n(s)} = G_n'(s) = G_n(s) e^{i\beta_n} \tag{17}$$

Because $e^{i\beta_n}$ is an unitary operator, $\|y_n\|_2 = \|w_n\|_2$ where $\|\cdot\|_2$ is the Euclidean norm of (·).

C. Feedback Control Design Procedure

The design objectives of the control are twofold. First the estimated domain of attraction Ω_{V_Γ} is to be maximized. Because $\Omega_{V_\Gamma} \subseteq \{x : Cx \in \Gamma\}$, the goal is to design the control parameters such that $k_{\min}$ is minimized, thus maximizing the set Γ given in Eq. (16). Second, to reduce actuator requirements, it is desired to have k_n.

Given that the system is in the appropriate feedback structure in Fig. 1, the design procedure evolves from achieving the design objectives subject to satisfying the conditions of the modified circle criterion. This results in a constrained optimization problem of the parameter $\beta \in [0 \text{ deg}, 360 \text{ deg})$ such that $k_{\min}$ is minimized subject to the modified circle criterion conditions.

An example is presented to illustrate the design utility of the modified circle condition. For a given operating point $\bar{\phi}_3$, it is desired to minimize $k_{\min}$, thus maximizing Γ in Eq. (16). To illustrate the effect of the control parameter β, consider the case with $\bar{\phi}_3 = 0.45$ with $k_{\max} = 25$ for the system given in Eq. (17). Shown in Fig. 7 is frequency response of $G'(s)$ with $\beta = 0°$. For absolute stability $G'(s)$ must encircle the disc $D(k_{\min}, k_{\max} = 25)$ defined from the sector bounds. Thus, the smallest $k_{\min}$ that satisfies the circle criterion is $k_{\min} = 21.05$. Recall that β is a spatial phase shift; that is, it rotates the frequency response plot in the s-plane about the origin. Thus, with the same $k_{\max} = 25$ by selecting $\beta = -31$ deg, the frequency response $G'(s)$ is rotated such that it encircles the disc $D(k_{\min}, k_{\max} = 25)$, as shown in Fig. 8 with a $k_{\min} = 18.19$. Therefore, the parameter β can be chosen graphically to minimize $k_{\min}$. This example illustrates the role the control parameter β has in maximizing the set Γ.

D. Design Example

An extension of the design procedure presented in the previous section can be used to design a fixed parameter controller for several operating points. The design procedure is illustrated by an example. Consider the case with several operating points. The first spatial mode open-loop transfer function $G_1'(s, \bar{\phi})$ is unstable (one unstable pole) for $\bar{\phi} = 0.46, 0.455, 0.45$, and 0.448 and stable for $\bar{\phi} = 0.48$ and 0.47. Using the controller design procedure of the preceding section, β_1 is designed such that $k_{\min}(\bar{\phi})$ is minimized for each operating point. Because the controller parameters are constant, the upper sector bound $k_{\max}$ is set equal to k_1, which is the minimum value of $k_{\max}$ such that $\tilde{\Psi}(t, y) \le k_{\max}$. Therefore, the frequency responses for the unstable plants must encircle the disc $D(k_{\min}, k_{\max} = k_1)$ and frequency responses for the stable plants must lie to the right of $-1/k_1$.

Shown in Fig. 7 are the frequency responses for $G_1'(s)$ for the controller phase shift of $\beta_1 = 0$ deg. Notice that for a fixed controller structure where $\beta_1 = \text{constant}$, minimizing $k_{\min}(\bar{\phi})$ cannot be satisfied for all operating points simultaneously. For example, $\beta_1 = -32$ deg produces the smallest possible $k_{\min}$ for $\bar{\phi} = 0.448$ and $\beta_1 = -30$ deg produces the smallest possible $k_{\min}$ for $\bar{\phi} = 0.455$ as shown in Fig. 7. Therefore, the controller phase shift could be chosen based on which operating points are most significant for the particular application. This limitation could be alleviated by using a gain-scheduling approach. For this example, β_1 was designed to be $\beta_1 = -30$ deg. From Fig. 7 the controller gain k_1 must satisfy $k_1 > 21.35$, which is the smallest gain to simultaneously satisfy the encirclement condition for all unstable operating points in the set. The gain k_1 for this example is chosen to be 25 and $k_{\max} = 25$. Using Theorem 2 with $k_{\max} = 25$ and $\beta_1 = -30$ deg, the norm-bounded subset of Ω_{V_Γ} is shown in Fig. 9 for the circle criterion. This norm-bounded subset is the estimated domain of attraction representing a measure of achievable performance subject to the actuator

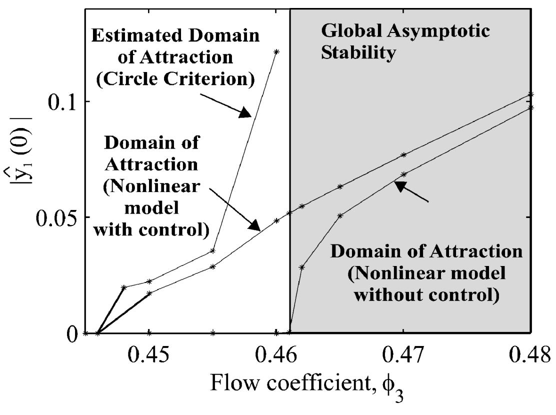

Fig. 10 Norm-bounded subset of Ω_{V_Γ}.

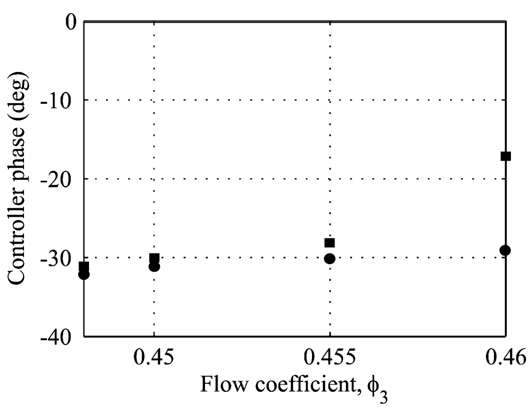

Fig. 11 Optimal controller phase predicted by the circle criterion, ○, and found through simulation of nonlinear system, □.

nonlinearity. Note that if the actuator nonlinearity is neglected, linear stability theory predicts that all the operation points considered are globally asymptotic stable.

Shown in Fig. 10 is a comparison of the estimated domain of attraction from the circle criterion and those found through simulation (using Simulink and MATLAB®) of the nonlinear model with and without control. This plot reveals that the circle criterion overestimates the domains of attraction of the full nonlinear compressor model, particularly at open-loop stable operation points and operating points nearby where the circle criterion predicts global asymptotic stability. The differences can be attributed to nonlinearities of the compressor model that are neglected in the circle criterion analysis. As the region about the linearization is expanded, the nonlinear terms of the compressor model become more prominent. This is one of the difficulties that arises in attempting to increase the domain of attraction for a nonlinear system utilizing a linearized model. Despite these differences, an increase in performance of the nonlinear model across all operating points was achieved with the controller designed using the circle criterion as shown in Fig. 10.

A comparison of the optimal controller phase found through simulation of the nonlinear compressor model and that designed using the modified circle criterion for several operating points is shown in Fig. 11. The comparison reveals that the modified circle criterion design corresponded well to the optimal controller phase at lower flow coefficients. However, as the flow coefficient approaches open-loop stable operating points, the designed and optimal controller phase begins to deviate where the nonlinear effects of the compressor model are more prominent.

VI. Conclusion

Presented in this paper is a controller design methodology for rotating stall that includes memoryless sector-bounded actuator nonlinearities (i.e., actuator saturation) defined in the spatial domain. The circle criterion was extended to accommodate the spatial domain model structure thereby resulting in a graphical solution used to facilitate the design process. The benefit of the graphical solution is that it allows actuator nonlinearities to be accounted for while using classical linear controller design techniques during the design. The application of the circle criterion illustrates the limitations on performance as a direct result of the spatial domain actuation nonlinearity. The complex gain control law was then incorporated into the analysis. From the analysis, a methodology was provided for the design of the control parameters k_n and β_n in the presence of limited control authority. The comparison between the circle criterion analysis with the results of the simulated nonlinear model revealed that the neglected nonlinear compressor dynamics cause the circle criterion to overestimate the domains of attraction. However, the control law developed using this design procedure was shown to increase the performance of the nonlinear compressor model across all operating points.

In this study a low-speed compressor was considered so that it could be assumed that the spatial modes were decoupled for the linearized model resulting in SISO systems. Doing so allows the graphical interpretation of the modified circle criterion to be applied. Although only the case $n = 1$ was presented, the criteria can be applied to the other spatial modes as well.

Appendix: Modified Circle Criterion Proof

Lemma 1: Let $Z(s)$ be a $p \times p$ rational transfer function matrix, and suppose $\det[Z(s) + Z^T(-s)]$ is not identically zero. Then, $Z(s)$ is strictly positive real if and only if

1) $Z(s)$is Hurwitz,
2) $Z(\infty) + Z^T(\infty) > 0$, and
3) $Z(j\omega) + Z^T(-j\omega) > 0,\ \forall\, \omega \in R$.

Proof: See Khalil.[12]

Lemma 2: Let $G_{RC}(s)$ be a real coefficient rational transfer function. Then, everywhere $G_{RC}(s)$ is analytic, $G_{RC}(s) = G^*_{RC}(s)$ where $*$ is the complex conjugate transpose operator.

Proof: Because $G_{RC}(s)$is a real coefficient rational transfer function it can be written in the following form:

$$G_{RC}(s) = \frac{\prod_k (s + a_k) \prod_l (s + c_l + i d_l)(s + c_l - i d_l)}{\prod_m (s + b_m) \prod_n (s + e_n + i f_n)(s + e_n - i f_n)}$$

where $a_k, b_m, c_l, d_l, e_n, f_n \in R$. Therefore,

$$G_{RC}(s^*) = \frac{\prod_k \left(s^* + a_k\right) \prod_l \left(s^* + c_l + i d_l\right)\left(s^* + c_l - i d_l\right)}{\prod_m \left(s^* + b_m\right) \prod_n \left(s^* + e_n + i f_n\right)\left(s^* + e_n - i f_n\right)}$$

$$G_{RC}(s^*) = \frac{\prod_k (s + a_k)^* \prod_l (s + c_l - i d_l)^*(s + c_l + i d_l)^*}{\prod_m (s + b_m)^* \prod_n (s + e_n - i f_n)^*(s + e_n + i f_n)^*}$$

$$G_{RC}(s^*) = G^*_{RC}(s)$$

Lemma 3: Consider the following complex coefficient rational transfer functions $G(s) = G_R(s) + i G_I(s)$ and $F(s) = G_R(s) - i G_I(s)$ where $G_R(s)$ and $G_I(s)$ are real coefficient rational transfer functions. Then $\mathrm{Re}\{G(s^*)\} = \mathrm{Re}\{F(s)\}$ everywhere that $G_R(s)$ and $G_I(s)$ are analytic where $*$ is the complex conjugate transpose operator and $\mathrm{Re}\{\cdot\}$ denotes the real part of $\{\cdot\}$. Furthermore, for some $\kappa \in R$, if $\mathrm{Re}\{G(j\omega)\} > \kappa\ \forall\, \omega \in R$ then $\mathrm{Re}\{F(j\omega)\} > \kappa\ \forall\, \omega \in R$ provided $G(s)$ is analytic on the imaginary axis.

Proof: Note that $G^*(s) \neq G(s^*)$. However, from Lemma 2, $G^*_R(s) = G_R(s^*)$ and $G^*_I(s) = G_I(s^*)$ because $G_R(s)$ and $G_I(s)$ are real coefficient rational transfer functions. Then,

$$\begin{aligned} G(s^*) &= G_R(s^*) + i G_I(s^*) = G^*_R(s) + i G^*_I(s) \\ &= [G_R(s) - i G_I(s)]^* \\ &= F^*(s) \end{aligned}$$

This implies $\text{Re}\{G(s^*)\} = \text{Re}\{F(s)\}$. It follows directly if $\text{Re}\{G(j\omega)\} > \kappa\ \forall\,\omega \in R$, then $\text{Re}\{F(j\omega)\} > \kappa\ \forall\,\omega \in R$.

Lemma 4: Consider the nonlinearity

$$\Psi(t, y) = \tilde{\Psi}(t, y)y$$

where $\tilde{\Psi}(\cdot,\cdot) : [0, \infty) \times R^2 \to R^1$ is a memoryless nonlinearity. If $\tilde{\Psi}(\cdot,\cdot)$ satisfies $0 \le k_{\min} < \tilde{\Psi}(t, y) < k_{\max}\ \forall\, t \ge 0$ on a set $\Gamma \subseteq R^2$ that is connected and contains the origin, then the nonlinearity $\Psi(t, y)$ satisfies the sector condition on Γ with $K_{\min} = k_{\min} I$ and $K_{\max} = k_{\max} I$.

Proof: Applying Definition 1 requires that

$$[\Psi(t, y) - K_{\min} y]^T [\Psi(t, y) - K_{\max} y] \le 0, \qquad \forall\, t \ge 0, \qquad \forall y \in \Gamma$$

Therefore, it follows directly that

$$[\Psi(t, y) - K_{\min} y]^T [\Psi(t, y) - K_{\max} y]$$

$$= \left[\tilde{\Psi}(t, y) - k_{\min}\right]^T \left[\tilde{\Psi}(t, y) - k_{\max} y\right] y y^T \le 0$$

on the set Γ because $0 \le k_{\min} < \tilde{\Psi}(t, y) < k_{\max}\ \forall\, y \in \Gamma$ and $yy^T \ge 0,\ \forall\, y$.

Proof of Theorem 3: To prove Theorem 3, first an equivalent real-coefficient multivariable absolute stability problem is constructed. Second, it is necessary to show that if either condition 1 or 2 of Theorem 3 is satisfied, then the multivariable circle criterion is satisfied for the equivalent real coefficient system.

The SISO complex coefficient feedback system Eqs. (12)–(14) can be represented as the real coefficient 2×2 MIMO feedback system, Eqs. (1)–(3). This realization is accomplished by defining the new state variable $\tilde{x}(t) = [\text{Re}\{x(t)\}, \text{Im}\{x(t)\}]^T$, the new output variable $\tilde{y}(t) = [\text{Re}\{y(t)\}, \text{Im}\{y(t)\}]^T$, and the new input variable $\tilde{u}(t) = [\text{Re}\{u(t)\}, \text{Im}\{u(t)\}]^T$ where $\text{Re}\{\cdot\}$ and $\text{Im}\{\cdot\}$ represent the real and imaginary component of $\{\cdot\}$, respectively. The resulting system equations are

$$\dot{\tilde{x}}(t) = \tilde{A}\tilde{x}(t) + \tilde{B}\tilde{u}(t)$$

$$\tilde{y}(t) = \tilde{C}\tilde{x}(t)$$

$$\tilde{u}(t) = -\tilde{\Psi}(t, \tilde{y})\tilde{y}$$

where

$$\tilde{A} = \begin{bmatrix} \text{Re}\{A\} & -\text{Im}\{A\} \\ \text{Im}\{A\} & \text{Re}\{A\} \end{bmatrix}, \qquad \tilde{B} = \begin{bmatrix} \text{Re}\{B\} & -\text{Im}\{B\} \\ \text{Im}\{B\} & \text{Re}\{B\} \end{bmatrix}$$

$$\tilde{C} = \begin{bmatrix} \text{Re}\{C\} & -\text{Im}\{C\} \\ \text{Im}\{C\} & \text{Re}\{C\} \end{bmatrix}$$

and $\tilde{\Psi}(\cdot,\cdot) : [0, \infty) \times R^2 \to R^1$. Similarly the Laplace transform of linear dynamics of the complex coefficient SISO system (12) and (13) given by $Y(s) = G(s)U(s) = [G_R(s) + iG_I(s)]U(s)$ can be written in terms of the new variables as

$$\tilde{Y}(s) = \tilde{G}(s)\tilde{U}(s) = \tilde{C}(sI - \tilde{A})^{-1}\tilde{B}\tilde{U}(s)$$

$$= \begin{bmatrix} G_R(s) & -G_I(s) \\ G_I(s) & G_R(s) \end{bmatrix} \tilde{U}(s)$$

Furthermore, by applying Lemma 4, the nonlinearity $\Psi(t, \tilde{y}) = \tilde{\Psi}(t, \tilde{y})\tilde{y}$ is shown to be sector bounded on Γ with $K_{\min} = k_{\min} I$ and $K_{\max} = k_{\max} I$, because $0 \le k_{\min} < \tilde{\Psi}(t, y) < k_{\max}$ on Γ. Using this equivalent real coefficient feedback system, the remaining portion of the proof proceeds by showing that conditions of Theorem 3 satisfy the multivariable circle criterion (Theorem 1) for this equivalent system.

Proof for Condition 1 of Theorem 3: With the equivalent real-coefficient multivariable system defined, it is sufficient to show that the multivariable circle criterion (Theorem 1) is satisfied for the equivalent real-coefficient system if the following conditions on $G(s)$ are met: 1) $G(s)$ is Hurwitz and strictly proper and 2) $\text{Re}\{G(j\omega)\} > -1/k_{\max}$ for $k_{\min} = 0$ and $k_{\max} > 0$. For the circle criterion to be satisfied $\tilde{Z}(s) = I + K\tilde{G}(s)$ must be Hurwitz and strictly positive real where $K = kI = k_{\max} I$ and $\tilde{G}(s)$ is the real coefficient transfer function matrix representation of $G(s)$.

First, $\det[\tilde{Z}(s) + \tilde{Z}^T(-s)]$ is not identically zero because a strictly proper $G(s)$ implies $G(\infty) \to 0$ and $G(-\infty) \to 0$. This implies $\tilde{G}(\infty) \to 0$ and $\tilde{G}(-\infty) \to 0$, thus $\tilde{Z}(\infty) \to I$ and $\tilde{Z}(-\infty) \to I$. As a result, $\det[\tilde{Z}(\infty) + \tilde{Z}^T(-\infty)] \to 2I$, and therefore the conditions of Lemma 1 can be used to show that $\tilde{Z}(s)$ is strictly positive real and Hurwitz. To conclude the proof it is necessary to show that Theorem 3 satisfies the three conditions of Lemma 1:

Satisfying condition 1 of Lemma 1: A Hurwitz $G(s)$ implies $\tilde{G}(s)$ is Hurwitz, which implies $\tilde{Z}(s) = I + K\tilde{G}(s)$ is Hurwitz.

Satisfying condition 2 of Lemma 1: A strictly proper $G(s)$ implies $G(\infty) \to 0$, which implies $\tilde{G}(\infty) \to 0$, thus $\tilde{Z}(\infty) \to I$. Therefore, $[\tilde{Z}(\infty) + \tilde{Z}^T(\infty)] \to 2I > 0$.

Satisfying condition 3 of Lemma 1: Let $G(s) = G_R(s) + iG_I(s)$ and $F(s) = G_R(s) - iG_I(s)$ where $G_R(s)$ and $G_I(s)$ are real coefficient transfer functions. Let $G_R(s) = a + ib$ and $G_I(s) = c + id$ where $a, b, c, d \in R$ are dependent on s.

A hermitian matrix M is positive definite if and only if all the eigenvalues of M are greater than zero.[16] Clearly $\tilde{Z}(s) + \tilde{Z}^*(s)$ is hermitian; therefore, $\tilde{Z}(j\omega) + \tilde{Z}^*(j\omega) > 0$ if and only if all the eigenvalues of $\tilde{Z}(s) + \tilde{Z}^*(s)$ are greater than zero for $s = j\omega\,\forall\,\omega \in R$.

To show this, consider

$$\tilde{Z}(s) + \tilde{Z}^*(s) = I + kI \begin{bmatrix} a + ib & -c - id \\ c + id & a + ib \end{bmatrix} + I$$

$$+ kI \begin{bmatrix} a - ib & c - id \\ -c + id & a - ib \end{bmatrix}$$

$$\tilde{Z}(s) + \tilde{Z}^*(s) = 2k \begin{bmatrix} \dfrac{1}{k} + a & -id \\ id & \dfrac{1}{k} + a \end{bmatrix}$$

Eigenvalues of $\tilde{Z}(s) + \tilde{Z}^*(s)$ are the values of λ satisfying

$$\begin{vmatrix} \lambda - \dfrac{1}{k} - a & id \\ -id & \lambda - \dfrac{1}{k} - a \end{vmatrix} = 0$$

Let $\gamma = \lambda - \dfrac{1}{k}$, then

$$\begin{vmatrix} \gamma - a & id \\ -id & \gamma - a \end{vmatrix} = \gamma^2 - 2a\gamma + a^2 - d^2 = 0$$

then

$$\gamma_1 = a + d, \qquad \gamma_2 = a - d$$

Therefore, $\lambda > 0 \Leftrightarrow \gamma > -1/k \Leftrightarrow a + d = \text{Re}\{F(s)\} > -1/k$ and $a - d = \text{Re}\{G(s)\} > -1/k$. Using Lemma 3, $\text{Re}\{G(j\omega)\} > -1k, \forall\,\omega$ implies $\tilde{Z}(j\omega) + \tilde{Z}^*(j\omega) > 0,\ \forall\,\omega$.

Proof for Condition 2 of Theorem 3: Similarly, it is sufficient to show that the multivariable circle criterion (Theorem 1) is satisfied for the equivalent real-coefficient system if the following conditions on $G(s)$ are met: 1) $G(s)$ is strictly proper and 2) the polar plot of $G(j\omega)$ does not enter the disk $D(k_{\min}, k_{\max})$ and encircles the disk counterclockwise n times, where n is the number of poles of $G(s)$ with positive real parts. For the multivariable circle criterion to be satisfied, $\tilde{G}_T(s)$ (defined in Theorem 1) must be Hurwitz and $\tilde{Z}_T(s) = I + K\tilde{G}_T(s)$ must be Hurwitz and strictly positive real where $K = kI = (k_{\max} - k_{\min})I$ and $\tilde{G}_T(s)$ is the real coefficient transfer function matrix representation of $G_T(s) = G(s)[I + k_{\min} G(s)]^{-1}$. Because $G(s)$ is strictly proper, $G_T(s)$ is strictly proper. Also $G_T(s)$ is Hurwitz because $G(s)$ has n number of unstable poles and $G(j\omega)$ encircles the $-1/k_{\min}$ point

n times counterclockwise. Therefore, $\tilde{G}_T(s)$ is strictly proper and Hurwitz.

The proof follows the same process as for condition 1 of Theorem 3. The resulting condition for the circle criterion to be satisfied is $\mathrm{Re}\{G_T(j\omega)\} > -1/(k_{\max} - k_{\min}),\ \forall\,\omega$. This condition can be rewritten as $\mathrm{Re}\{[1 + k_{\max}G(j\omega)][1 + k_{\min}G(j\omega)]^{-1}\} > 0,\ \forall\,\omega$ and is satisfied if $G(j\omega)$ does not enter the disk $D(k_{\min}, k_{\max})$.

References

[1]Protz, J. M., "Nonlinear Active Control of Rotating Stall and Surge," Master's Thesis, Dept. of Aeronautics and Astronautics, Massachusetts Institute of Technology, June 1997.

[2]Day, I., "Stall Inception in Axial Flow Compressors," *Journal of Turbomachinery*, Vol. 115, Jan. 1993, pp. 1–9.

[3]Behnken, R., "Nonlinear Control and Modeling of Rotating Stall in an Axial Flow Compressor," Ph.D. Dissertation, Dept. of Mechanical Engineering, California Institute of Technology, Sept. 1997.

[4]D'Andrea, R., Behnken, R., and Murray, R., "Rotating Stall Control of an Axial Flow Compressor Using Pulsed Air Injection," *Journal of Turbomachinery*, Vol. 119, Oct. 1997, pp. 742–752.

[5]Moore, F. K., and Greitzer, E., "A Theory of Post-Stall Transients in Axial Compression Systems: Part I—Development of Equations," *Journal of Engineering for Gas Turbines and Power*, Vol. 108, Jan. 1986, pp. 68–76.

[6]Epstein, A., Williams, J. F., and Greitzer, E., "Active Suppression of Aerodynamic Instabilities in Turbomachines," *Journal of Propulsion and Power*, Vol. 5, No. 2, 1989, pp. 204–211.

[7]Haynes, J., Hendricks, G., and Epstein, A., "Active Stabilization of Rotating Stall in a Three-Stage Axial Compressor," *Journal of Turbomachinery*, Vol. 116, April 1994, pp. 226–239.

[8]Paduano, J., Epstein, A., Valavani, L., Longley, J., Greitzer., E., and Guenette, G., "Active Control of Rotating Stall in a Low-Speed Axial Compressor," *Journal of Turbomachinery*, Vol. 115, Jan. 1993, pp. 48–56.

[9]Vo, H. D., and Paduano, J., "Experimental Development of a Jet Injection Model for Rotating Stall Control," American Society of Mechanical Engineers, Paper No. 98-GT-308, June 1998.

[10]Hendricks, G., and Gysling, D., "Theoretical Study of Sensor-Actuator Schemes for Rotating Stall Control," *Journal of Propulsion and Power*, Vol. 10, No. 1, 1994, pp. 101–109.

[11]Aizerman, M., and Gantmacher, F., *Absolute Stability of Regulator Systems*. Holden-Day, San Francisco, 1964.

[12]Khalil, H. K., *Nonlinear Systems*, Prentice Hall, Upper Saddle River, NJ, 1996.

[13]Chiang, H., and Thorp, J., "Stability Regions of Nonlinear Dynamical Systems: A Constructive Approach," *IEEE Transactions on Automatic Control*, Vol. 34, No. 12, 1989, pp. 1229–1241.

[14]Haddad, W., Kapila, V., and Chellabonina, V., "Guaranteed Domains of Attraction for Multivariable Lure Systems via Open Lyapunov Surfaces," *International Journal of Robust and Nonlinear Control*, Vol. 7, No. 10, 1997, pp. 935–949.

[15]Mansoux, C., Gysling, D., Setiawan, J., and Paduano, J., "Distributed Nonlinear Modeling and Stability Analysis of Axial Compressor Stall and Surge," *Proceedings of the American Control Conference*, IEEE Pub., Piscataway, NJ, 1994, pp. 2305–2316.

[16]Ogata, K., *Modern Control Engineering*, 2nd ed., Prentice Hall, Englewood Cliffs, NJ, 1990.